

Current-assisted Raman activation of the Higgs mode in superconductors

Matteo Puviani,¹ Lukas Schwarz,¹ Xiao-Xiao Zhang,² Stefan Kaiser,^{1,3} and Dirk Manske^{1,*}

¹Max Planck Institute for Solid State Research, 70569 Stuttgart, Germany

²Department of Physics and Astronomy & Stewart Blusson Quantum Matter Institute, University of British Columbia, Vancouver, Canada BC V6T 1Z4

³4th Physics Institute and Research Center SCoPE, University of Stuttgart, 70569 Stuttgart, Germany

(Dated: June 18, 2020)

The Higgs mode in superconductors is a scalar mode without electric or magnetic dipole moment. Thus, it is commonly believed that its excitation is restricted to a nonlinear two-photon Raman process. However, recent efforts have shown that a linear excitation in the presence of a supercurrent is possible, resulting in a new resonant enhancement at $\Omega = 2\Delta$ with the driving light frequency Ω and the energy of the Higgs mode 2Δ . This is in contrast to the usual $2\Omega = 2\Delta$ resonance condition found in nonlinear third-harmonic generation experiments. In this communication, we show that such a linear excitation can still be described as an effective Raman two-photon process, with one photon at $\omega = 2\Delta$ and one virtual photon at $\omega = 0$ which represents the dc supercurrent. At the same time we demonstrate that a straightforward infrared activation with a single photon excitation is negligible. Moreover, we give a general context to our theory, providing an explanation for how the excitation of the Higgs mode in both THz quench and drive experiments can be understood within a conventional difference-frequency generation or sum-frequency generation process, respectively. In such a picture, the observed new resonance condition $\Omega = 2\Delta$ is just a special case. With the same approach, we further discuss another recent experiment, where we find a suppression of odd order higher harmonics in the presence of a dc supercurrent.

Introduction. Light excitation of collective modes in condensed matter physics is typically realized due to an infrared or Raman coupling of light to the system. This corresponds to a one- or two-photon process, i.e. a linear or a nonlinear coupling. If the mode does not have a dipole moment, a linear activation is forbidden, such that the only allowed process is due to the nonlinear Raman effect. This is true for the Higgs mode in superconductors, which is a collective oscillation of the amplitude of the order parameter [1, 2]. Its observation so far was realized either in a quench-probe [3] or a periodic driven setup [4–6], where in both cases the coupling of light to the superconductor can be described by a quadratic nonlinear effective Raman process. Due to this nonlinear coupling, light of frequency Ω drives the system effectively with a frequency of 2Ω leading to enforced 2Ω oscillations of the order parameter. A tuning of the effective driving frequency to the energy of the Higgs mode at 2Δ leads to an enhancement of the oscillations and a resonance peak in the spectrum at $2\Omega = 2\Delta$. This second-harmonic component in the order parameter oscillation translates into third-harmonic generation (THG) in emission and the resonance is observable in the emitted THG signal [7, 8].

Recent studies have shown that a linear coupling of light to the condensate is possible in the presence of a supercurrent [9]. Hereby, the current provides a momentum to the center of mass of the condensate, such that the scalar Higgs mode can be excited with a single photon. With this, the equilibrium forbidden linear driving with

the frequency Ω is now possible due to the breaking of equilibrium inversion symmetry and enforces the order parameter to oscillate at just Ω . As a result, the first-harmonic oscillation of the order parameter shows a new resonance condition at $\Omega = 2\Delta$. In an emission experiment, second-harmonic generation (SHG) would occur and the new resonance is then observable in the emitted SHG signal. Furthermore, the effect is also visible in the linear response and indeed, an enhancement in the optical conductivity was observed in the superconductor NbN, which was driven by a dc supercurrent [10].

In this communication we extend previous theoretical studies of current- and light-driven superconductors, providing a new interpretation of the experimental findings. We argue that this coupling should not be understood as an infrared activation of the Higgs mode in a single photon process but rather as a current-assisted Raman interaction, where the excitation is still realized with a two-photon coupling to the condensate. In the present work, we exploit this effect to interpret experimental results and to predict further experimental outcomes. In this two-photon process, one photon is at the energy $\omega = \Omega$ and the other photon is a virtual photon with $\omega = 0$ given by the dc supercurrent. We find that a single photon infrared activation is negligible compared to such an effective Raman process.

Distinguishing the current-assisted Higgs excitation as being either infrared or Raman-like is fundamental and has important implications for designing future experiments to excite and investigate the Higgs mode in the flourishing field of Higgs spectroscopy. As there is an ongoing debate on how this activation can be understood [10–12], this communication suggests a consistent inter-

* d.manske@fkf.mpg.de

pretation, which was not given in the previous theoretical study [9]. Furthermore, the description of the excitation process is more general and allows to describe the usual nonlinear two-photon activation of the Higgs mode, or more generally any collective mode, in quench or drive experiments with a sum-frequency generation (SFG) or difference-frequency generation (DFG) scheme. Within this picture, the current-assisted excitation just represents a special case with one photon energy set to zero.

Current-assisted Raman. To describe the coupling of light to current-carrying superconductors, we start with a phenomenological description using a Lagrangian of Ginzburg-Landau type. For the complex superconducting order parameter $\psi(\mathbf{r}, t)$ coupled to a gauge field $A_\mu = (\phi, \mathbf{A}(t))$ where we choose $\phi = 0$, the time- and space-dependent Lagrangian reads

$$\mathcal{L} = (D_\mu \psi)^* (D^\mu \psi) - V(\psi) - \frac{1}{4} F_{\mu\nu} F^{\mu\nu}, \quad (1)$$

where the potential $V(\psi) = \alpha|\psi|^2 + \frac{\beta}{2}|\psi|^4$ has the shape of a Mexican hat in the superconducting state with $\alpha < 0$. The gauge covariant derivative reads $D_\mu = \partial_\mu + ieA_\mu$ with the effective charge e and the electromagnetic field tensor $F_{\mu\nu} = \partial_\mu A_\nu - \partial_\nu A_\mu$. We are interested in small fluctuations around the groundstate value $|\psi_0| = \sqrt{-\alpha/\beta}$, thus, we use an ansatz $\psi(\mathbf{r}, t) = (\psi_0 + H(\mathbf{r}, t))e^{i\theta(\mathbf{r}, t)}$ to describe amplitude (Higgs) fluctuations H and phase (Goldstone) fluctuations θ . Neglecting higher orders and constant terms, the resulting Lagrangian for the fluctuations reads

$$\begin{aligned} \mathcal{L} = & \left(\partial_\mu H - ie \left(A_\mu + \frac{1}{e} \partial_\mu \theta \right) (\psi_0 + H) \right) \\ & \times \left(\partial^\mu H + ie \left(A^\mu + \frac{1}{e} \partial^\mu \theta \right) (\psi_0 + H) \right) \\ & + 2\alpha H^2 - \frac{1}{4} F_{\mu\nu} F^{\mu\nu}. \end{aligned} \quad (2)$$

We now consider the situation in which the superconductor is at the same time driven by a homogeneous light field with frequency Ω and in which a dc supercurrent is injected. Thus, we write the vector potential as $\mathbf{A}(t) = \mathbf{A}_0 e^{i\Omega t} + \mathbf{Q}/e$, where the condensate momentum \mathbf{Q} is defined by the gauge invariant current $\mathbf{j} = en_s \hbar/m(e\mathbf{A} - \nabla\theta) = en_s \hbar/m\mathbf{Q}$, with n_s being the superconducting density, m and e the electron effective mass and charge, respectively [13]. Due to the Anderson-Higgs mechanism, the phase fluctuations can be gauged out by a choice of $\chi = -\theta$, where $\psi' = \psi e^{i\chi}$ and the redefined vector potential $A'_\mu = A_\mu - \frac{1}{e} \partial_\mu \chi$ [14]. Dropping the primes, the Lagrangian then reads

$$\begin{aligned} \mathcal{L} = & (\partial_\mu H)(\partial^\mu H) + 2\alpha H^2 - \frac{1}{4} F_{\mu\nu} F^{\mu\nu} \\ & + e^2 \psi_0^2 A_\mu A^\mu + 2e^2 \psi_0 A_\mu A^\mu H. \end{aligned} \quad (3)$$

The term $\mathcal{L}_{\text{int}} = 2e^2 \psi_0 A_\mu A^\mu H$ describes the coupling between the gauge field and Higgs and reads explicitly

$$\mathcal{L}_{\text{int}} = 2e^2 \psi_0 (A^2 H + \frac{2}{e} \mathbf{Q} \mathbf{A} H + \frac{1}{e^2} \mathbf{Q}^2 H). \quad (4)$$

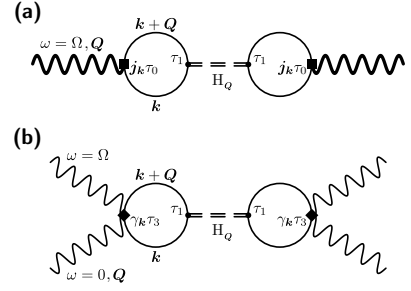


Figure 1. Feynman diagrams describing excitation of Higgs mode in current-carrying state with condensate momentum \mathbf{Q} and light frequency Ω . a) Single-photon infrared excitation with first-order derivative vertex interaction $j_{\mathbf{k}} \propto \partial_{\mathbf{k}} \epsilon_{\mathbf{k}}$. b) Effective Raman excitation with second-order derivative vertex interaction $\gamma_{\mathbf{k}} \propto \partial_{\mathbf{k}}^2 \epsilon_{\mathbf{k}}$. Wiggly, wiggly bold, solid and double dashed lines represent photon, photon interacting with current, electron and Higgs propagator.

We observe that for finite \mathbf{Q} a linear coupling term arises. The equation of motion for the amplitude fluctuations H at $q = 0$ reads

$$\partial_t^2 H = 2\alpha H + e^2 \psi_0 A^2 + 2e\psi_0 \mathbf{Q} \mathbf{A} + \psi_0 \mathbf{Q}^2 \quad (5)$$

and the stationary solution is easily obtained as

$$H = \frac{\psi_0 \mathbf{Q}^2}{\omega_{\text{H}}^2} - \frac{2e\psi_0 \mathbf{Q} A_0}{\Omega^2 - \omega_{\text{H}}^2} e^{i\Omega t} - \frac{e^2 \psi_0 A_0^2}{4\Omega^2 - \omega_{\text{H}}^2} e^{2i\Omega t}, \quad (6)$$

where the energy of the Higgs mode $\omega_{\text{H}}^2 = -2\alpha$ is obtained for $A_\mu = 0$. From the microscopic theory it is known that $\omega_{\text{H}} = 2\Delta$ [1]. For $\mathbf{Q} = 0$, only the nonlinear driven oscillations exists with $\omega = 2\Omega$ resonating at $2\Omega = 2\Delta$. For $\mathbf{Q} \neq 0$, a linear coupling is possible resulting in an oscillation with $\omega = \Omega$ resonating at $\Omega = 2\Delta$. Using similar arguments, this result of linear coupling was first derived in [9]. In general, one could have included an additional nonrelativistic Gross-Pitaevskii-like term $\propto \psi^* D_0 \psi$ in addition to the relativistic Klein-Gordon-like description of the dynamics. However, it is known that in the nonrelativistic case, there is no distinct Higgs mode as amplitude and phase channel are coupled [2]. Despite the fact that a current would support a particle-hole breaking term, its contribution cannot be large. Otherwise, a resonance at ω_{H} is not explainable.

With the most general Lagrangian approach we have demonstrated that the coupling of light to the Higgs mode in a superconductor can be linear in the presence of a supercurrent. A normal dissipative current would not be sufficient, as a nonzero superfluid momentum has to be present to break time-reversal symmetry. In order for this effect to be induced by a normal current, electrons would have to interact at the same time with the light and the Cooper pairs of the condensate. A minimal scheme representing the interaction of one photon with the moving condensate suggested by the Lagrangian description is the infrared activation of the Higgs mode, depicted in

Fig. 1(a). Thus, we calculate the current-current correlation function in the presence of the Higgs mode using this diagram. The amplitude of the transmitted electric field is given by $E(\mathbf{Q}, \Omega) \propto \mathbf{Q} \mathbf{A} |\chi_{jj}^H(\mathbf{Q}, \Omega)|$ [8, 15, 16]. The susceptibility $\chi_{jj}^H(\mathbf{q}, \Omega)$ is given by

$$\chi_{jj}^H(\mathbf{q}, \Omega) = H(\mathbf{q}, \Omega) \chi_{j1}^2(\mathbf{q}, \Omega) = -\frac{\chi_{j1}^2(\mathbf{q}, \Omega)}{2/V + \chi_{11}(\mathbf{q}, \Omega)} \quad (7)$$

with the condensate pairing interaction V and the Higgs propagator $H(\mathbf{q}, \Omega) = -(2/V + \chi_{11}(\mathbf{q}, \Omega))^{-1}$. We use the indices of the susceptibility to denote the vertices of the corresponding bubbles: j for the current channel $j_k \tau_0$ and 1 for the amplitude channel τ_1 . The vertices are written as matrices in Nambu space [17] and τ_i are the Pauli matrices. The susceptibility $\chi_{j1}(\mathbf{q}, \Omega)$ reads after analytic continuation $i\omega_n \rightarrow \Omega$ of the expression

$$\begin{aligned} \chi_{j1}(\mathbf{q}, i\omega_n) &= \sum_{\mathbf{k}} j_{\mathbf{k}} f_{\mathbf{k}} \iint d\omega_1 d\omega_2 \frac{\Delta_{\mathbf{k}} \omega_2 + \Delta_{\mathbf{k}+\mathbf{q}} \omega_1}{2E_{\mathbf{k}} E_{\mathbf{k}+\mathbf{q}}} \\ &\times \frac{n_F(\omega_1) - n_F(\omega_2)}{\omega_1 - \omega_2 + i\omega_n} [\delta(\omega_1 - E_{\mathbf{k}}) - \delta(\omega_1 + E_{\mathbf{k}})] \\ &\times [\delta(\omega_2 - E_{\mathbf{k}+\mathbf{q}}) - \delta(\omega_2 + E_{\mathbf{k}+\mathbf{q}})], \end{aligned} \quad (8)$$

with $j_{\mathbf{k}} = \partial_{\mathbf{k}} \epsilon_{\mathbf{k}}$, electron dispersion $\epsilon_{\mathbf{k}}$, energy gap $\Delta_{\mathbf{k}}$, gap symmetry $f_{\mathbf{k}}$, quasiparticle energy $E_{\mathbf{k}} = \sqrt{|\Delta_{\mathbf{k}}|^2 + \epsilon_{\mathbf{k}}^2}$ and Fermi function n_F . Details of the calculation can be found in the supplemental material [18]. In the limit $\mathbf{q} \rightarrow 0$, the term $\Delta_{\mathbf{k}}(\omega_1 + \omega_2)$ is nonzero only when $\omega_1 = \omega_2 = E_{\mathbf{k}}$, but in this case, $n_F(E_{\mathbf{k}}) - n_F(E_{\mathbf{k}}) = 0$, thus, $\chi_{j1}(\mathbf{q} = 0, \Omega) = 0$ is identically zero. For finite but small $\mathbf{q} = \mathbf{Q}$, the contribution of this diagram is still small. For very large \mathbf{Q} , the contribution gets comparable to the Raman process, which we will discuss next. However, it is no longer peaked at $\Omega = 2\Delta$, but is shifted to higher energies reflecting the quadratic dispersion of the Higgs mode [7]. This is shown in more detail in the supplemental material [18]. As no such shift is observed experimentally, the value of \mathbf{Q} must be small. Using parameters from the experiment in [10], we estimate the value of the supercurrent induced momentum in units of the lattice constant $1/a_0 = 10^8 \text{ cm}^{-1}$ as $Qa_0 = \frac{m}{en_s \hbar} j a_0 \approx 3.7 \cdot 10^{-4}$ with electron mass $m = m_e$ and charge e , superfluid density $n_s = 5.4 \cdot 10^{20} \text{ cm}^{-3}$ and current density $j = 3.7 \cdot 10^6 \text{ A/cm}^2$. Thus, the contribution from the infrared diagram in the current-carrying state is negligible.

Since such an infrared linear coupling has difficulties to explain the resonance at $\Omega = 2\Delta$, we considered a microscopic description using BCS theory with inversion symmetry breaking due to the supercurrent. The BCS Hamiltonian within Anderson pseudospin formulation [19] can be written as $H = \sum_{\mathbf{k}} \mathbf{b}_{\mathbf{k}} \sigma_{\mathbf{k}}$ with the definition of the pseudospin $\sigma_{\mathbf{k}} = \frac{1}{2} \Psi_{\mathbf{k}}^\dagger \boldsymbol{\tau} \Psi_{\mathbf{k}}$, where $\Psi_{\mathbf{k}}^\dagger = (c_{\mathbf{k}\uparrow}^\dagger, c_{-\mathbf{k}\downarrow})$ is the Nambu-Gorkov spinor and $\boldsymbol{\tau}$ the vector of Pauli matrices. The pseudomagnetic field $\mathbf{b}_{\mathbf{k}}$ for a real gap $\Delta_{\mathbf{k}} = \Delta f_{\mathbf{k}}$, driving amplitude

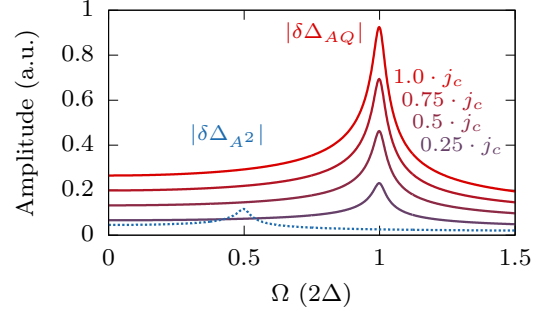


Figure 2. Amplitudes of the induced gap oscillations from Eq. (10) for s -wave superconductor in units of $\omega_H = 2\Delta$ with $f(\varphi) = 1$ and varying current strength using values of the experiment [10] (see supplemental material for details and numerical values). Resonances of the driving light with the Higgs mode appear at $2\Omega = 2\Delta$ without (blue) and at $\Omega = 2\Delta$ (red) with supercurrent.

$\mathbf{A}(t) = \mathbf{A}_0 \sin(\Omega t)$ and current induced momentum \mathbf{Q} reads $\mathbf{b}_{\mathbf{k}}^\top(t) = (-2\Delta_{\mathbf{k}}(t), 0, \epsilon_{\mathbf{k}-e\mathbf{A}(t)-\mathbf{Q}} + \epsilon_{\mathbf{k}+e\mathbf{A}(t)+\mathbf{Q}})$. Neglecting the imaginary part of the gap, which is unimportant for our discussion, the gap equation expressed in the pseudospin picture reads $\Delta(t) = V \sum_{\mathbf{k}} f_{\mathbf{k}} \langle \sigma_{\mathbf{k}}^x \rangle(t)$ where the function $f_{\mathbf{k}}$ describes the symmetry of the gap and V is the pairing interaction. We expand the z -component of the pseudomagnetic field in powers of \mathbf{A} and obtain

$$\mathbf{b}_{\mathbf{k}}^z \approx 2\epsilon_{\mathbf{k}} + \sum_{ij} \partial_{ij}^2 \epsilon_{\mathbf{k}} \left(e^2 A_i A_j + 2e A_i Q_j + Q_i Q_j \right), \quad (9)$$

where ∂_{ij}^2 is the partial derivative with respect to k_i and k_j . Hereby, the first order terms $\pm \sum_i \partial_i \epsilon_{\mathbf{k}} (e A_i + Q_i)$ cancel due to parity, corresponding to the vanishing of the infrared diagram in Fig. 1(a) for $\mathbf{q} \rightarrow 0$. However, as for the Lagrangian description developed before, for finite \mathbf{Q} , a new term linear in \mathbf{A} arises. With this approach we see from the expansion in Eq. (9) that both the linear and quadratic couplings are proportional to the second derivative of the band dispersion, giving rise to the Raman vertex coefficient $\gamma_{\mathbf{k}}$ in the effective mass approximation [20]. In addition, the coupling occurs in the z -component of the pseudomagnetic field, i.e. the τ_3 channel, reflecting a Raman coupling [15, 21]. Thus, the pseudospin description contains more information than the Lagrangian formulation, and no assumptions on the nature of the coupling has been made.

We now proceed by evaluating the linearized Bloch equations $\partial_t \sigma_{\mathbf{k}} = \mathbf{b}_{\mathbf{k}} \times \sigma_{\mathbf{k}}$ for small deviations $\delta\Delta(t)$ from the equilibrium value Δ , from which the observable higher-order current $j^H(t) \propto \delta\Delta(t) A(t)$ can be obtained [7]. The solution reads $\delta\Delta(t) = \delta\Delta_{A^2}(t) + \delta\Delta_{AQ}(t) + \delta\Delta_{Q^2}(t)$ where each term arises from one of the expression $\propto A_i A_j$, $\propto A_i Q_j$ and $\propto Q_i Q_j$ in Eq. (9). Assuming $\epsilon_{\mathbf{k}} = \epsilon(|\mathbf{k}|)$ and $f_{\mathbf{k}} = f(\varphi)$ depending only on the polar angle φ and neglecting the trivial term $\delta\Delta_{Q^2}$, the remaining two terms

read explicitly in the long-time limit

$$\delta\Delta_{A^2}(t) \propto \frac{e^2 A_0^2 \Omega \cos(2\Omega t)}{\int d\varphi f^2 \sqrt{4\Delta^2 f^2 - \Omega^2} \sin^{-1}\left(\frac{\Omega}{2\Delta|f|}\right)}, \quad (10a)$$

$$\delta\Delta_{AQ}(t) \propto \frac{4eA_0 Q \Omega \sin(\Omega t)}{\int d\varphi f^2 \sqrt{4\Delta^2 f^2 - \Omega^2} \sin^{-1}\left(\frac{\Omega}{2\Delta|f|}\right)}. \quad (10b)$$

The first term $\delta\Delta_{A^2}(t)$ describes the 2Ω oscillations of the order parameter resonating at $2\Omega = 2\Delta$ which are induced by the usual quadratic coupling [7]. The second term $\delta\Delta_{AQ}(t)$ describes the equilibrium forbidden Ω oscillations of the order parameter with a new resonance at $\Omega = 2\Delta$, which is only present for finite condensate momentum Q . The amplitudes of both terms are shown exemplary in Fig. 2 for s -wave symmetry with $f(\varphi) = 1$ and different strengths for the current using values of the experiment [10] (see supplemental material [18] for parameter details and an evaluation for d -wave). One observes that the resonance peak in the current-activated term is comparable in size or even exceeds the usual quadratic term in the range of experimental reachable values.

In a diagrammatic representation, we might describe both processes, the quadratic and linear coupling, with an effective Raman vertex as shown in Fig. 1(b). For the quadratic coupling, each incident photon line corresponds to one photon of frequency $\omega = \Omega$, resulting in the $2\Omega = 2\Delta$ resonance. For the linear coupling, one incident photon corresponds to the light photon with $\omega = \Omega$, whereas the second incident photon line is a virtual photon at $\omega = 0$, representing the dc supercurrent. An evaluation of the diagram shows that it is equivalent to the linearized solution in the pseudospin formalism (see supplemental material [18] for details). This mechanism also has an analogy to the Higgs excitation in the superfluid phase of ultracold bosons [22]. Here, a nonzero expectation value of a boson operator due to the superfluid condensate enables a linear coupling to the vector potential similar to the finite Q of the supercurrent. Thus, such a current-assisted Raman diagram can explain the $\Omega = 2\Delta$ resonance in the current-carrying state.

Based on this interpretation, we can also understand a recent experiment [11], where a strong THz field dynamically induces a dc component due to an effective asymmetric pulse shape resulting from nonlinear effects. The situation can be described in analogy to the here discussed case by a current-assisted Raman activation. To make this explicit, we model this experiment in accordance to [11] using an asymmetrically shaped vector potential $A(t) \propto A_0(\sin(\Omega t) + \kappa)/(1 + \kappa)$, where $\kappa \neq 0$ determines the asymmetry, and solve the Bloch equations numerically (see supplemental material [18] for details). The vector potential and the resulting even and odd order higher harmonics in the gap oscillations can be seen in Fig. 3 (blue curves). In order to demonstrate the equivalence between the dynamically induced dc component by the asymmetric vector potential and the external dc current, we consider the situation where both effects are

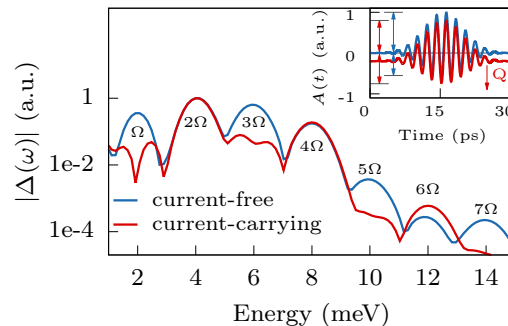


Figure 3. Spectrum of gap oscillations induced by an asymmetrically shaped vector potential as observed in [11] (blue). Note that in the current-free state, the positive amplitude is larger than the negative amplitude (as indicated by the blue arrows), while in the current-carrying state, the symmetry is partly restored (red arrows). The asymmetric pulse dynamically induces a dc supercurrent component which allows even and odd order higher harmonics. If an external supercurrent with momentum Q is applied with opposite direction, the odd order higher harmonics get suppressed (red curve). Details about the calculation can be found in the supplemental material [18].

included. If an additional external supercurrent with momentum Q is applied in opposite direction to the dynamically driven supercurrent, i.e. $A(t) + Q/e$ with $Q < 0$, the inversion symmetry can be partially restored, giving rise to a suppression of the odd order higher harmonics (red curves). Thus, the current-assisted Raman activation can successfully explain this experiment and an extension of the setup allows to demonstrate the equivalence of the dynamically induced dc component and an external dc current.

SFG and DFG for Higgs mode. With this insight, we can summarize and classify the possible known excitation schemes of Higgs modes as sketched in Fig. 4. In the impulsive excitation of a Higgs mode, a short intense THz pulse quenches the Mexican hat potential of the complex superconducting order parameter. That process follows the scheme of impulsive stimulated Raman scattering [21, 23] shown in Fig. 4(a). The Higgs mode is excited via the difference-frequency of the photons Ω_1 and Ω_2 that stem from the same pulse. The required frequencies are within the bandwidth of the ultrashort broadband THz pulse. Experimentally, the free Higgs oscillations observed in NbN [3] are excited this way.

Instead of a difference-frequency process between the incoming photons, it is also possible to excite the Higgs mode via a sum-frequency process to excite Raman active modes [24] as shown in Fig. 4(b). In analogy to Fig. 4(a), this can be a quench of the system, where the two photons stem from the same pulse. Furthermore, the 2Ω oscillations of the driven Higgs mode in NbN [4], Nb₃Sn [11, 25] and in cuprates [6, 26], as well as the driven Leggett mode in MgB₂ [12] can be also understood in this way. In these cases, the two photons $\Omega_1 = \Omega_2 = \Omega$ have the same frequency leading to the experimentally observed

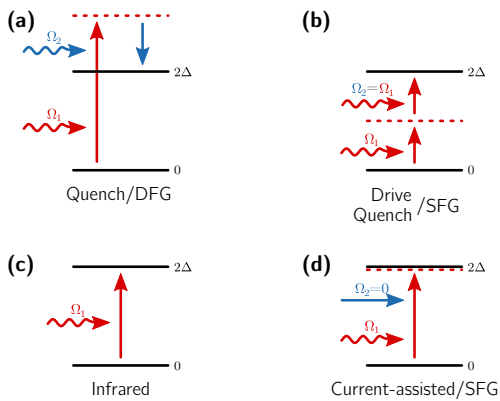


Figure 4. Different excitation schemes of Higgs mode. a) Excitation due to quench with two-photon Raman difference-frequency generation (DFG) process. The frequencies Ω_1 and Ω_2 are within the bandwidth of the quench pulse. b) Driving of Higgs mode with two-photon Raman sum-frequency generation (SFG) process. The frequencies of the photons are equal $\Omega_1 = \Omega_2 = \Omega$. Alternatively, a quench can be implemented as a SFG process as well, where the two frequencies are within the bandwidth of the quench pulse. c) One-photon infrared process. d) Two-photon current-assisted Raman process with $\Omega_1 = \Omega$ and $\Omega_2 = 0$ reflecting a special case of a SFG process.

second harmonic generation and the $2\Omega = 2\Delta$ resonance condition. This two-photon Raman process is described by the $\propto A_i A_j$ term in Eq. (9).

In contrary, an infrared excitation is a one photon absorption process by coupling to a dipolar moment shown in Fig. 4(c). However, as we have discussed in this communication, the current-driven superconductor does not

change the character of the Higgs mode. The current rather gives rise to a new $\propto A_i Q_j$ term in Eq. (9) that describe an effective Raman two-photon excitation. In addition to the photon $\Omega_1 = \Omega$, the current takes the role of a photon with $\Omega_2 = 0$. As such, the current-driven case can be understood in analogy with the SFG or DFG Raman processes, leading to $\Omega_1 \pm \Omega_2 = \Omega$ and the new $\Omega = 2\Delta$ resonance condition shown in Fig. 4(d).

Conclusion. In short, we provide an alternative explanation for the recent experimental conclusion that in the presence of a supercurrent the Higgs mode becomes infrared active. Our theory shows that in this case, the activation of the Higgs mode is an effective Raman process (SFG or DFG), where one of the photons is a virtual photon at $\omega = 0$. On the other hand we demonstrate that an infrared activation is negligible.

Our theory properly describes the experimental observation of the appearance of the Higgs mode in the linear THz spectrum of NbN in the presence of a dc current [10]. Moreover, it explains the appearance of the Ω oscillation in the THz driven Nb₃Sn in addition to the 2Ω terms and the higher odd order interference terms [11, 25], resulting from a dynamically driven dc current. With a model calculation we propose an extension to this experiment which allows to confirm the equivalence of a dynamically driven dc supercurrent and our theory by a suppression of odd order higher harmonics in the gap oscillations. Furthermore, our results are not restricted to conventional *s*-wave superconductors and thus, will guide further current-assisted experiments also on unconventional superconductors.

Acknowledgements. We thank the Max Planck-UCB-UTokyo Center for Quantum Materials for fruitful collaborations and financial support.

-
- [1] C. Varma, Higgs Boson in Superconductors, *J. Low. Temp. Phys.* **126**, 901 (2002).
- [2] D. Pekker and C. Varma, Amplitude/Higgs Modes in Condensed Matter Physics, *Annu. Rev. Condens. Matter Phys.* **6**, 269 (2015).
- [3] R. Matsunaga, Y. I. Hamada, K. Makise, Y. Uzawa, H. Terai, Z. Wang, and R. Shimano, Higgs Amplitude Mode in the BCS Superconductors Nb_{1-x}Ti_xN Induced by Terahertz Pulse Excitation, *Phys. Rev. Lett.* **111**, 057002 (2013).
- [4] R. Matsunaga, N. Tsuji, H. Fujita, A. Sugioka, K. Makise, Y. Uzawa, H. Terai, Z. Wang, H. Aoki, and R. Shimano, Light-induced collective pseudospin precession resonating with Higgs mode in a superconductor, *Science* **345**, 1145 (2014).
- [5] R. Matsunaga, N. Tsuji, K. Makise, H. Terai, H. Aoki, and R. Shimano, Polarization-resolved terahertz third-harmonic generation in a single-crystal superconductor NbN: Dominance of the Higgs mode beyond the BCS approximation, *Phys. Rev. B* **96**, 020505 (2017).
- [6] H. Chu, M.-J. Kim, K. Katsumi, S. Kovalev, R. D. Dawson, L. Schwarz, N. Yoshikawa, G. Kim, D. Putzky, Z. Z. Li, H. Raffy, S. Germanskiy, J.-C. Deinert, N. Awari, I. Ilyakov, B. Green, M. Chen, M. Bawatna, G. Cristiani, G. Logvenov, Y. Gallais, A. V. Boris, B. Keimer, A. P. Schnyder, D. Manske, M. Gensch, Z. Wang, R. Shimano, and S. Kaiser, Phase-resolved higgs response in superconducting cuprates, *Nat. Commun.* **11**, 1793 (2020).
- [7] N. Tsuji and H. Aoki, Theory of Anderson pseudospin resonance with Higgs mode in superconductors, *Phys. Rev. B* **92**, 064508 (2015).
- [8] T. Cea, C. Castellani, and L. Benfatto, Nonlinear optical effects and third-harmonic generation in superconductors: Cooper pairs versus Higgs mode contribution, *Phys. Rev. B* **93**, 180507 (2016).
- [9] A. Moor, A. F. Volkov, and K. B. Efetov, Amplitude Higgs Mode and Admittance in Superconductors with a Moving Condensate, *Phys. Rev. Lett.* **118**, 047001 (2017).
- [10] S. Nakamura, Y. Iida, Y. Murotani, R. Matsunaga, H. Terai, and R. Shimano, Infrared Activation of the Higgs Mode by Supercurrent Injection in Superconducting NbN, *Phys. Rev. Lett.* **122**, 257001 (2019).
- [11] X. Yang, C. Vaswani, C. Sundahl, M. Mootz, L. Luo, J. H. Kang, I. E. Perakis, C. B. Eom, and J. Wang, Lightwave-driven gapless superconductivity and forbidden quantum beats by terahertz symmetry breaking, *Nature Photonics*

- 13**, 707–713 (2019).
- [12] F. Giorgianni, T. Cea, C. Vicario, C. P. Hauri, W. K. Withanage, X. Xi, and L. Benfatto, Leggett mode controlled by light pulses, *Nature Physics* **15**, 341–346 (2019).
- [13] M. Buzzi, G. Jotzu, A. Cavalleri, J. I. Cirac, E. A. Demler, B. I. Halperin, M. D. Lukin, T. Shi, Y. Wang, and D. Podolsky, Higgs-mediated optical amplification in a non-equilibrium superconductor, [arXiv:1908.10879](https://arxiv.org/abs/1908.10879) (2019).
- [14] P. W. Anderson, Plasmons, Gauge Invariance, and Mass, *Phys. Rev.* **130**, 439 (1963).
- [15] T. P. Devereaux and R. Hackl, Inelastic light scattering from correlated electrons, *Rev. Mod. Phys.* **79**, 175 (2007).
- [16] M. Udina, T. Cea, and L. Benfatto, Theory of coherent-oscillations generation in terahertz pump-probe spectroscopy: From phonons to electronic collective modes, *Phys. Rev. B* **100**, 165131 (2019).
- [17] Y. Nambu, Quasi-Particles and Gauge Invariance in the Theory of Superconductivity, *Phys. Rev.* **117**, 648 (1960).
- [18] See Supplemental Material at [URL] for details about the calculation.
- [19] P. W. Anderson, Random-Phase Approximation in the Theory of Superconductivity, *Phys. Rev.* **112**, 1900 (1958).
- [20] T. P. Devereaux, D. Einzel, B. Stadlober, R. Hackl, D. H. Leach, and J. J. Neumeier, Electronic Raman scattering in high- T_c superconductors: A probe of $d_x^2-y^2$ pairing, *Phys. Rev. Lett.* **72**, 396 (1994).
- [21] T. E. Stevens, J. Kuhl, and R. Merlin, Coherent phonon generation and the two stimulated Raman tensors, *Phys. Rev. B* **65**, 144304 (2002).
- [22] S. D. Huber, E. Altman, H. P. Büchler, and G. Blatter, Dynamical properties of ultracold bosons in an optical lattice, *Phys. Rev. B* **75**, 085106 (2007).
- [23] Y. Yan, E. B. Gamble, and K. A. Nelson, Impulsive stimulated scattering: General importance in femtosecond laser pulse interactions with matter, and spectroscopic applications, *The Journal of Chemical Physics* **83**, 5391 (1985).
- [24] S. Maehrlein, A. Paarmann, M. Wolf, and T. Kampfrath, Terahertz Sum-Frequency Excitation of a Raman-Active Phonon, *Phys. Rev. Lett.* **119**, 127402 (2017).
- [25] C. Vaswani, M. Mootz, C. Sundahl, D. H. Mudiyansele, J. H. Kang, X. Yang, D. Cheng, C. Huang, R. H. J. Kim, Z. Liu, L. Luo, I. E. Perakis, C. B. Eom, and J. Wang, Terahertz second-harmonic generation from lightwave acceleration of symmetry-breaking nonlinear supercurrents, *Phys. Rev. Lett.* **124**, 207003 (2020).
- [26] K. Katsumi, N. Tsuji, Y. I. Hamada, R. Matsunaga, J. Schneeloch, R. D. Zhong, G. D. Gu, H. Aoki, Y. Gallais, and R. Shimano, Higgs Mode in the d -Wave Superconductor $\text{Bi}_2\text{Sr}_2\text{CaCu}_2\text{O}_{8+x}$ Driven by an Intense Terahertz Pulse, *Phys. Rev. Lett.* **120**, 117001 (2018).